Dissertation

Analysis and Processing of Signals in Laser Bathymetry

Ausgeführt zum Zwecke der Erlangung des akademischen Grades eines
Doktors der technischen Wissenschaften (Dr.techn.)

Unter der Leitung von
Univ.-Prof. Dipl.-Ing. Dr.techn. Norbert Pfeifer

E 120
Department für Geodäsie und Geoinformation
Forschungsbereich Photogrammetrie

Eingereicht an der Technischen Universität Wien
Fakultät für Mathematik und Geoinformation

von
Dipl.-Ing. Roland Schwarz
Matrikelnummer: 07925314
Österreich

Wien, 2. Februar 2021

Unterschrift

Dissertation

Analysis and Processing of Signals in Laser Bathymetry

A thesis submitted in fulfillment of the academic degree of
"Doktors der technischen Wissenschaften (Dr.techn.)" *)

under the supervision of
Univ.-Prof. Dipl.-Ing. Dr.techn. Norbert Pfeifer

E 120
Department of Geodesy and Geoinformation
Research Unit Photogrammetry

Research conducted at TU Wien
Faculty of Mathematics and Geoinformation

by
Dipl.-Ing. Roland Schwarz
Matriculation number: 07925314
Austria

Vienna, February 2, 2021

Signature

*) comparable to the Doctor of Engineering Sciences

Supervisor: Prof. Dr. Norbert Pfeifer
TU Wien
Department of Geodesy and Geoinformation
Wiedner Hauptstraße 8-10, 1040 Vienna, Austria
E-Mail: norbert.pfeifer@geo.tuwien.ac.at

Signature

Referee: Prof. Dr.-Ing. Uwe Stilla
Technische Universität München
Fakultät für Luftfahrt, Raumfahrt und Geodäsie
Arcisstr. 21, 80333 Munich, Germany
E-Mail: stilla@tum.de

Signature

Referee: Assoc. Prof. Dr. Sagi Filin
Technion - Israel Institute of Technology
Transportation and Geo-Information Engineering
Haifa 32000, Israel
E-Mail: filin@technion.ac.il

Signature

Erklärung zur Verfassung der Arbeit
Author's Statement

Hiermit erkläre ich, dass ich diese Arbeit selbstständig verfasst habe, dass ich die verwendeten Quellen und Hilfsmittel vollständig angegeben habe und dass ich die Stellen der Arbeit - einschließlich Tabellen, Karten und Abbildungen -, die anderen Werken oder dem Internet im Wortlaut oder dem Sinn nach entnommen sind, auf jeden Fall unter Angabe der Quelle als Entlehnung kenntlich gemacht habe.

I hereby declare, that I independently drafted this manuscript, that all sources and references used are correctly cited and that the respective parts of this manuscript including tables, maps and figures - which were included from other manuscripts or the internet, either semantically or syntactically -, are made clearly evident in the text and all respective sources are correctly cited.

Dipl.-Ing. Roland Schwarz
Lobenhauerngasse 11/2/20
A-1170 Wien
Österreich

(Unterschrift / Signature)

Contents

Acknowledgements

Normally you write a dissertation at the end of your academic education before you enter professional life. But life is not always straightforward, and a professionally successful life can be achieved without academic blessings. But eventually you realize that the academic dimension is much more than just a nice outfit. For me it became a synonym for the honest and serious discussion of scientific questions. In my whole, professionally quite satisfying life, I have never lost the desire to discuss questions that go beyond their mere usefulness.

You can consider yourself lucky if you meet Univ.-Prof. Dipl.-Ing. Dr.techn. Norbert Pfeifer, head of the research unit of photogrammetry of the TU Wien, in this situation, although you are close to retirement age. It was during a project-related work for which I temporarily had to move my desk to the technical university, when I re-infected myself with the academic virus. Norbert you encouraged me to pursue my desire to begin a dissertation despite my advanced age. For this I thank you, Norbert, and for giving me such good advice and support along the way!

You can consider yourself at least as lucky if your employer shows understanding for the fact that it is an important aspect of a successful life for you to continue your academic path. I feel a deep gratitude to my employer Univ.Doz. Univ.Prof. Dipl.-Ing. Dr.techn. Johannes Riegl, founder and head of RIEGL Laser Measurement Systems, because he showed understanding for my project. I am equally grateful to CTO Dipl.-Ing. Dr.techn. Andreas Ullrich that I was able to turn to current operational research and development issues for the practical parts of my dissertation.

The collaboration with Dipl.-Ing. Dr.techn. Martin Pfennigbauer, head of Riegl Research, was and still is a great pleasure for me. It would not have happened without his sense for a rigorous scientific approach, without losing the focus on practical applicability.

The number of people engaged in laser bathymetry research in a country without direct access to the sea is not very large. I therefore feel very fortunate that I was privileged to work with Senior Scientist Dipl.-Ing. Dr.techn. Gottfried Mandlburger from whom I learned a lot about the practical aspects of scientific work.

I also thank all my female and male colleagues for putting up with my sometimes hair-splitting discussions.

Last but not least I thank my wife Karin. I thank you, dear Karin, for patiently tolerating my absence while I was working on my dissertation. When I have finished my dissertation, we will watch "Dr. Who" again together on TV. Big word of honor!

Abstract

Airborne laser bathymetry is a remote sensing technique for the mapping of underwater topography. Compared to topograhic airborne laser scanning, light propagation in two media must be considered. An important difference also is that for use in bathymetry, only wavelengths of the laser in the visible range can be used, since light in the infrared range is practically unable to penetrate the water. The first generation of scanners for bathymetry came into use shortly after the invention of the LASER. Although in the beginning mainly only analog electronics was available for the evaluation of the signals, later the entire trace of the backscattered echo was recorded digitally. The advent of affordable computers finally opened the way to more complex signal processing.

For the determination of the elevation of the underwater bottom it is necessary to identify two significant time instants in the waveform. The first is when the light impulse enters the water and the second is when it hits the bottom. It is especially important to know the first moment, because from this moment on the impulse moves slower and in a different direction.

The standard method to identify an instant of time in a signal is by gaussian decomposition of the signal. Underwater, however, the method suffers from the problem that a lot of distributed small particles cause clutter that is hindering the exact decomposition. For a tenuous distribution of such particles the waveform is of exponential character. In this thesis I therefore introduce a model consisting of exponential segments that describe the effect of the particles and Dirac shaped pulses that describe the effect of discretely located scatterers. This description is however not sufficient yet to account for the received signal form. The exponential model has to be convolved with the system waveform to yield a correct representation of the received signal. By minimizing the difference of this representation and the measured data the parameters of the exponential model can be retrieved. I present a procedure, which I call exponential decomposition, by which the actual processing can be done. The effectiveness of the procedure is verified on the basis of data collected in a tributary of the Danube river. The correctness of the results is confirmed using GNSS surveyed control points.

An important aspect for the modeling of signals is that the model is physically correct. An underestimated effect in laser bathymetry is that pulsed light propagates more slowly than conventionally assumed. Since the effect in the context of laser bathymetry has not yet been discussed, I describe an experiment I performed that confirms the effect in its predicted magnitude.

Furthermore, I deal with the questions whether a single wavelength system is feasible and what the smallest measurable depth in laser bathymetry is.

Kurzfassung

Die luftgestützte Laser-Bathymetrie ist eine Fernerkundungstechnik zur Kartierung der Unterwassertopographie. Im Vergleich zum topographischen Airborne-Laserscanning ist die Lichtausbreitung in zwei Medien zu berücksichtigen. Ein wichtiger Unterschied besteht auch darin, dass für den Einsatz in der Bathymetrie nur Wellenlängen des Lasers im sichtbaren Bereich verwendet werden können, da Licht im Infrarotbereich praktisch nicht in das Wasser eindringen kann. Die erste Generation von Scannern für die Bathymetrie kam kurz nach der Erfindung des LASERS zum Einsatz. Während anfangs hauptsächlich nur analoge Elektronik für die Auswertung der Signale zur Verfügung stand, wurde später die gesamte Kurvenform des rückgestreuten Echos digital aufgezeichnet. Das Aufkommen erschwinglicher Computer öffnete schließlich den Weg zu komplexerer Signalverarbeitung.

Für die Bestimmung der Elevation des Unterwasserbodens ist es notwendig, zwei signifikante Zeitpunkte in der Wellenform zu identifizieren. Der erste ist der Zeitpunkt, zu dem der Lichtimpuls ins Wasser eintritt und der zweite der Zeitpunkt, zu dem er auf den Boden trifft. Es ist von besonderer Bedeutung, den ersten Moment zu kennen, denn von diesem Moment an bewegt sich der Impuls langsamer und in eine andere Richtung.

Die Standardmethode zur Identifizierung eines Zeitpunkts in einem Signal ist die Gauß'sche Zerlegung des Signals. Unter Wasser leidet die Methode jedoch unter dem Problem, dass viele verteilte kleine Partikel Störechos verursachen, die die genaue Zerlegung behindern. Solange die Verteilung solcher Teilchen nicht zu dicht ist hat die Wellenform exponentiellen Charakter. In dieser Arbeit stelle ich daher ein Modell vor, das aus Exponentensegmenten besteht, die die Wirkung der Teilchen beschreiben, und Dirac-förmigen Impulsen, die die Wirkung diskret angeordneter Streuer beschreiben. Diese Beschreibung ist jedoch noch nicht ausreichend, um die empfangene Signalform zu erklären. Das Exponentialmodell muss mit der Systemwellenform gefaltet werden, um eine korrekte Darstellung des empfangenen Signals zu erhalten. Durch Minimierung der Differenz zwischen dieser Darstellung und den gemessenen Daten können die Parameter des Exponentialmodells erhalten werden. Ich stelle eine Prozedur vor, die ich Exponentialzerlegung nenne, mit der die eigentliche Verarbeitung durchgeführt werden kann. Die Wirksamkeit des Verfahrens wird auf der Grundlage von Daten überprüft, die in einem Nebenfluss der Donau gesammelt wurden. Anhand von mittels GNSS-vermessenen Kontrollpunkten wird die Richtigkeit der Ergebnisse bestätigt.

Ein wichtiger Aspekt bei der Modellierung von Signalen ist, dass das Modell physikalisch korrekt ist. Ein unterschätzter Effekt in der Laser-Bathymetrie ist, dass sich gepulstes Licht langsamer ausbreitet als herkömmlich angenommen. Da der Effekt im Zusammenhang mit der Laser-Bathymetrie noch nicht diskutiert worden ist, beschreibe ich ein von mir durchgeführtes Experiment, das den Effekt in seiner vorhergesagten Größe bestätigt.

Darüber hinaus befasse ich mich mit den Fragen, ob ein Ein-Wellenlängensystem reali-

sierbar ist und was die kleinste messbare Tiefe in der Laser-Bathymetrie ist.

Acronyms

3D three dimensional 3

ALB airborne laser bathymetry 2, 3, 5, 6, 7, 13, 15, 20, 23, 26

ALS airborne laser scanning 2, 3, 5

dBCS differential backscatter cross section 13, 14, 25

DEM digital elevation model 1

GDC gaussian decomposition 5, 17, 22

GNSS global navigation satellite system 25

IR infra red 5, 20, 21

LASER light amplification by stimulated emission of radiation 2, 3, 5, 8, 10, 20, 21

LiDAR light detection and ranging 2, 3, 5, 7, 13, 14, 15, 20, 25

MME macroscopic Maxwell equations 3, 4, 5, 10, 15

RADAR radio detection and ranging 2

RTE radiative transfer equation 3, 4

RTM radiative transfer method 1

RTT radiative transfer theory 3, 4, 15

SDB satellite derived bathymetry 1

SONAR sound naviagtion and ranging 1

SVB surface volume bottom 14, 15, 22, 25, 26

SWFM system waveform 5, 13, 14, 17, 21, 25

TOF time of flight 2, 8

XDC exponential decomposition 5, 6, 13, 17, 19, 22, 25

1. Introduction

Bathymetry is the extension of topography into the underwater region. The name comes from the Greek word βαθύς (*bathus*), meaning "deep". Hydrography, although related, has a different purpose than bathymetry. The main task of bathymetry is the precise survey of the underwater terrain, while the purpose of hydrography is to provide information for the safety of navigation [8]. So, while the primary result of bathymetry is a digital elevation model (DEM) of the river bottom, the result of hydrography is a map of minimum depths. The early nautical recordings of such minimum depths were usually in private ownership of the respective navigator. It was the United Kingdom Hydrographic Office who made available the first official nautical charts in 1800 [9]. It may be worth noting that the apparent translation of the word "hydrography" into the German language, i.e., "Hydrographie" means something different in Austria, the Switzerland, and Germany. The meaning in Austria is defined in the standard "ÖNORM B 2400" while in Germany "DIN 18709-3" applies. Suffice it to say simply that both definitions have nothing to do with safety in shipping.

The tools of bathymetry and hydrography for probing the watercolumn are mostly the same. An early method of underwater sounding was by using a *lead line*. Contemporary water sounding techniques are based on either acoustic or electromagnetic waves. The standard technology to map the ocean still is by sound naviagtion and ranging (SONAR) because sound waves penetrate deeper into the water compared to electromagnetic waves. The history of SONAR is linked to the availability of electronics and dates back to the twenties of the 20th century [20]. Electromagnetic waves, on the other hand, virtually do not penetrate water significantly, with two exceptions: at very low frequencies and at frequencies of visible light. While wavelengths of about 15 km at low frequencies are unsuitable for measuring short distances, at wavelengths of 450 nm to 500 nm there is an optical window of minimum attenuation (Figure 1.1) through which light can penetrate down to a depth of approximately 1000 m into the sea. The presence of this window not only plays an important role for the existence of life, but it also enables the remote sensing of bathymetry by electromagnetic waves.

Both, passive and active methods have been developed to obtain bathymetry in the optical domain. Using the sun as source of radiation and a passive *multi-spectral* recording of reflected light, water depth can be derived because attenuation in water depends on the wavelength [23]. Such *multi-spectral* methods have been used succesfully for satellite derived bathymetry (SDB), but either they need a precise atmospheric correction, as is the case for the physics based radiative transfer method (RTM), or need in-situ depth data, as is the case for depth to colorindex correlations. A method to overcome these limitations for the case of SDB based on photogrammetry has been reported by Hodúl et al. [7].

Photo bathymetry is another passive method allowing to derive maps of the seafloor from aerial images. Under certain assumptions such as sufficient water clarity, limited depth, and a flat water surface, from air into water photogrammetry is feasible. Maas [15] investigates the accuracy potential of such a multi-media case of photogrammetry.

Although propagation of light beams in water has been studied [3] before the invention of light amplification by stimulated emission of radiation (LASER) active systems for optical bathymetry were feasible only after existence of the LASER. One of the earliest airborne laser bathymetry (ALB) systems has been described by Hickman and Hogg [6].

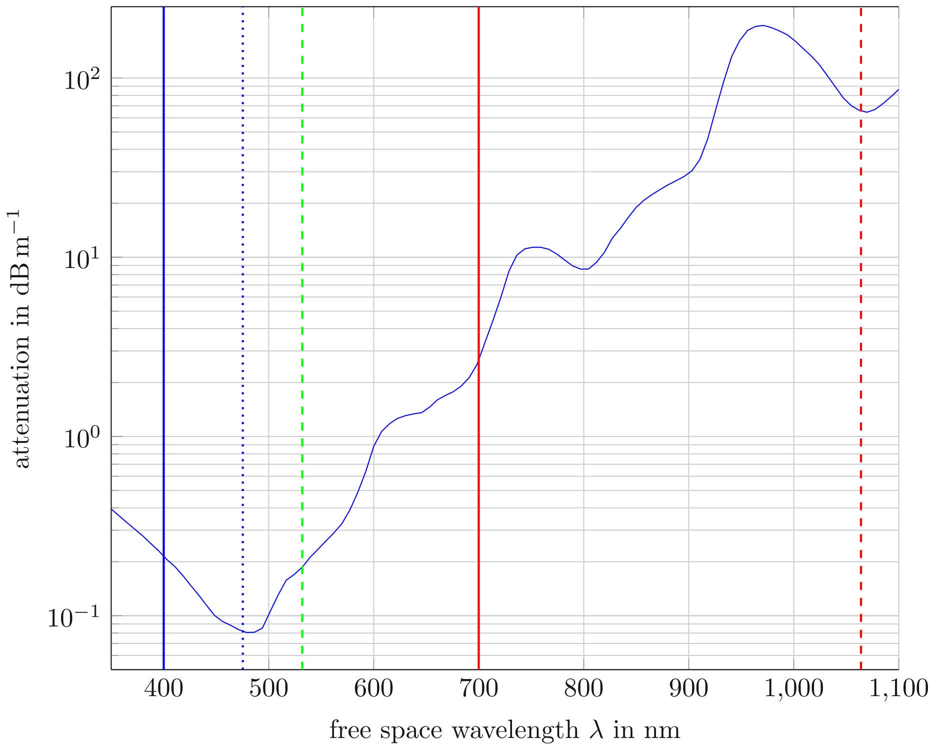

Figure 1.1.: Attenuation of pure water, calculated from data compiled by Segelstein [30], hosted on the internet by Polyanskiy [24]. Light visible to the human eye is between the blue and red solid lines. Minimum attenuation is at 475 nm marked by the dotted blue line. LASER wavelengths of 532 nm and 1064 nm are marked by green and red dashed lines.

Light detection and ranging (LiDAR) is an extension of radio detection and ranging (RADAR) [31] to the frequencies of light. The time of flight (TOF) between the emission of a pulse and the echo reflected from a target is used to calculate the range to the target by means of the known speed of light. Airborne laser scanning (ALS) employs a moving mirror system to direct the pulses to different points of a remote surface in rapid succession. While the technology was initially limited to military use, this changed in 1971 with the Apollo 15 mission, where a laser altimeter was used to map the surface of the moon. Apparently the adoption of ALS and ALB began at almost the same time. The early ALB systems were WREMAPS I in Australia, Optechs LARSEN-500 in Canada, AOL in the USA, and FLASH in Sweden [22]. Some time later, in 2011, the system VQ-820-G of company RIEGL from Austria became available. This system was representative for a new class of systems, the so called *topo-bathymetric* scanners. All these systems delivered sets of three dimensional (3D) coordinates of target points, also known as *point cloud*. Because more advanced signal processing methods are not always easy to implement as online methods, manufacturers began to record whole sections of the received signal and made them available for post-processing in addition to the point cloud. While already the LARSEN-500 was a system providing waveform recording, commercial *full-wave* systems were not available before 2004 [17].

One of the attractive features of LiDAR is the small wavelength of light that makes it possible to achieve narrow measuring beams with a small aperture size of the optics ultimately leading to a small illuminated area[1)] on the target. A very popular solid-state LASER source, is based on the Nd:YAG (neodymium-doped yttrium aluminium garnet) crystal as the lasing medium. These LASERs emit light with a free space wavelength of 1064 nm (infra red). As one can see (Fig. 1.1), even pure water attenuates the light by about $65\,\mathrm{dB\,m^{-1}}$ at this wavelength, making it essentially opaque. By adding a frequency-doubling crystal, however, light with a wavelength of 532 nm (visible green) can be obtained. The attenuation at this wavelength is only a fraction of a decibel per meter allowing light to penetrate into the water far enough for the purposes of ALB.

ALS and ALB, although very similar in many aspects, differ in that the LASER for ALB must penetrate two media, air *and* water. On the one hand this requires use of the already mentioned wavelength of 532 nm and on the other hand consideration of refraction, i.e. the change of beam propagation direction when passing from air to water. ALB systems also typically enforce a constant off-nadir angle of $\approx 20°$ for the measuring beam mainly to avoid receiver overload due to specular reflections from the water surface. Light propagation within the water body also differs significantly from propagation in air because scattering and attenuation in water is much more significant.

Guenther [4], one of the pioneers, has tried to answer many of the questions regarding ALB already back in 1985. Most importantly, he has discussed the problem of systematic overestimation of depth in ALB systems and also proposed a solution. He suggested a correction procedure based on the numerical solution of the radiative transfer equation (RTE) using Monte Carlo simulation. He has based his reasoning on the radiative transfer theory (RTT) because it was (and often still is) the standard tool for the study of propagation of light in scattering environments.

RTT has been criticized, however, for its purely phenomenological roots and its disconnectedness from modern physics. Mishchenko [19] in his essay “Directional radiometry and radiative transfer: The convoluted path from centuries-old phenomenology to physical optics” gives a comprehensive overview of the critique but he also shows that there is a "bridge" between RTT and the macroscopic Maxwell equations (MME) which are accepted as a fundamental physical law. The mathematical form of the RTE can be derived from the MME, some concepts, however, of the RTT need to be abandoned, such as the concepts of

[1)] The illuminated area often is called footprint.

independently scattering particles, elementary volume elements and photons as localized particles of light.

Models of bathymeric waveforms generally are either physically based or pragmatically motivated. Examples for the pragmatic approach are waveform shapes like the Gaussian [5], triangular [2] or quadrilateral [1] or a combination of multiple models [33]. Models based on physical considerations typically are based on the small angle scattering approximation solution of the RTE [11, 16, 13, 12].

In this thesis, however, I will use a physically motivated model based on the first order multiple scattering solution of the MME for a tenuous distribution of particles [10]. I will take this path, not only because of the criticism one can make of the RTT, but because the derivation of the model via the MME can explain the speed of pulse propagation in water in an explicit manner. From a pragmatic perspective, however, there is not much of a difference, because the functional form of the model will be essentially the same.

This thesis will continue in chapter 2 with the formulation of the specific objectives of this work and a few questions.

Chapter 3 presents a derivation of the first order multiple scattering model, similar to the derivation given by Ishimaru [10], but with explicit consideration of pulse propagation in dispersive media. The content of this chapter is not part of the already published articles.

A summary of the articles, constituting the main body of this thesis, is given in chapter 4 followed by chapter 5 for their discussion. The discussion section, however, will not simply repeat the respective sections of the papers but will concentrate on main issues and present an idea for future directions.

The work ends with the conclusions given in chapter 6.

2. Objectives and Questions

Much of the technology of ALB can also be found in topographic LiDAR. Indeed, newer systems show the ability to operate in a mixed environment of land and water. It turns out, however, that in either case understanding the waveform of the backscattered LASER echo is key to the successful processing of the raw data of such instruments. This work therefore focuses on the waveform. Because this work also focuses on bathymetry, i.e. the determination of the elevation of the bottom below water bodies, no emphasis was placed on a radiometrically calibrated result.

Adressed objectives:

Analysis of bathymetric waveforms. Bathymetric waveforms, in contrast to topographic waveforms, show distributed targets caused by particles in the water column, which must not be neglected. A frequently used model, originating from topographic ALS, is the Gaussian pulse shape. **Novel approach:** Based on the first order multiple scattering approximation from a solution of the MME the bathymetric waveform is modeled by a chain of exponential segments which are convolved with a per-sensor system waveform (SWFM).

Processing of bathymetric waveforms. For signal processing in ALB the gaussian decomposition (GDC) is often used, although it is actually insufficient. **Novel approach:** Taking advantage of the fact that the convolution of two sums of truncated exponentials can again be represented as the sum of truncated exponentials an algorithm is developed which I call exponential decomposition (XDC).

Specific questions:

Is single wavelength ALB feasible? Knowing the location of the water surface is required to apply refraction correction of the bottom points. The surface can either be measured by a second LASER in the infra red (IR) region or can be reconstructed from an analysis of the 3D-point statistics [18] below the surface. **Novel approach:** The exponential model used in this thesis exhibits a distinguished *leading edge*. The leading edge can be used to infer the water surface.

What is the minimum resolvable depth? The minimum resolvable depth depends on the effective width of the pulse, i.e. the SWFM, the refractive index of water, the off-nadir angle, and the ability of an algorithm, e.g. GDC or peak detection, to recognize separate targets.

Novel approach: Using XDC, introduced in this thesis, very closely spaced targets can be resolved.

How fast is light in water? The speed of light is required to accomplish refraction correction. The ALB literature generally uses the *phase velocity*, which is defined by the value of the refraction index at the laser wavelength. **Improvement of the standard approach:** Although known in other fields, the use of *group velocity* in the context of ALB is new, to the best of my knowledge, and reduces depth bias by about 1.5 %.

3. Waveforms in LiDAR Bathymetry

Remote sensing of water bodies obeys, of course, the well known general principles of LiDAR, in particular the radar equation is valid. However, certain characteristics of light propagation in water make it seem reasonable to review the formulas on which the model introduced in this work is based. In this context, two points will be addressed explicitly, which apply in principle in any medium, but require special attention in water: Firstly, this is the propagation velocity of the pulses which takes place with the so-called group velocity. This velocity, which is calculated using the derivative of instead just the value of the refractive index, is a bit smaller than the phase velocity commonly used in ALB. Secondly, it seems reasonable to explicitly review the physical considerations underlying the exponential model used in this thesis.

3.1. Radar Equation for Pulse Propagation

The model for ALB waveforms in this thesis is based on the first order multiple scattering approximation [10] valid for a volume density of scatterers of up to 0.1%. This means, that a scattered wave component as seen by the receiver is caused by a single scattering event only. Multiple scattering, however, is accounted for by considering absorption and scattering along the path.

The monostatic radar equation, under the first order multiple scattering assumption, for a monochromatic transmitter of frequency ω [2)] for a single scatterer is given by

$$\frac{P_R(\omega)}{P_T(\omega)} = A_R e^{-\gamma(r,\omega)} \frac{\sigma_b(\vec{r},\omega)}{4\pi r^2} e^{-\gamma(r,\omega)} \frac{G_T(\vec{e_r})}{4\pi r^2} \tag{3.1}$$

where $\vec{r}$ is a vector pointing from the sensor location to the scatterer, $r = |\vec{r}|$ is the scalar distance and $\vec{e_r} = \vec{r}/r$ the unit vector of direction. The average power received at the sensor location is $P_R(\omega)$, the receiver aperture is A_R, the average power transmitted is $P_T(\omega)$ and $G_T(\vec{e_r})$ is the transmitter gain in direction towards the scattering particle. The backscatter cross section of the scatterer is given by $\sigma_b(\vec{e_r},\omega)$ and generally depends on frequency as well. The optical distance γ is given by path integration

$$\gamma(\vec{r},\omega) = \int_{\mathcal{C}} \rho(\vec{s})\sigma_t(\vec{s},\omega)ds \tag{3.2}$$

along the optical path $\mathcal{C}$ from the sensor location to the scatterer at $\vec{r}$ of the total cross section σ_t weighted by the numerical density $\rho(\vec{r})$ of scatterers, i.e. the number of particles

2) $\omega = 2\pi f$ is the angular frequency.

per unit volume. The negative exponentiation of the optical path accounts for the signal attenuation due to multiple scattering in this model.

What is lost in (3.1) is the phase information of the received wave. For the proper understanding of pulse propagation, however, phase information is needed. Thus we use field quantities [3)], i.e. V_R, V_T, instead of power quantities, to express the radar equation in the form of the transfer function $H(\omega)$ by

$$H(\omega) = \frac{V_R(\omega)}{V_T(\omega)} = \frac{f_R(-\vec{e_r})f_P(-\vec{e_r},\vec{e_r})f_T(\vec{e_r})}{r^2} e^{-\gamma(r,\omega)} e^{-jk(\omega)2r} \quad , \tag{3.3}$$ [4)]

with

$$|f_R(-\vec{e_r})|^2 = A_R \quad , \quad |f_P(-\vec{e_r},\vec{e_r})|^2 = \frac{\sigma_b(\vec{r},\omega)}{4\pi} \quad \text{and} \quad |f_T(\vec{e_r})|^2 = \frac{G_T(\vec{e_r})}{4\pi} \quad . \tag{3.4}$$

We rewrite (3.3) as

$$H(\omega) = F(\omega)e^{-jk(\omega)2r} \tag{3.5}$$

with

$$F(\omega) = \frac{f_R(-\vec{e_r})f_P(-\vec{e_r},\vec{e_r})f_T(\vec{e_r})}{r^2} e^{-\gamma(r,\omega)} \quad . \tag{3.6}$$

Wavenumber $k(\omega)$, the number of oscillations per unit of length, determines the phase of the harmonic wave. It can be seen that the phase undergoes a rapid change depending on distance $2r$.

A LASER pulse $v(t)$ of a TOF system typically is a pulse of narrow bandwidth and can be modeled by using the so-called equivalent low pass pulse $s(t)$ [see e.g. 21]

$$v(t) = \mathrm{Re}\{s(t)e^{j\omega_0 t}\} \tag{3.7}$$

with ω_0 equal to the center frequency of the LASER source. The power of $v(t)$ is obtained by squaring

$$v^2(t) = \frac{1}{2}s(t)s^*(t) + \frac{1}{2}\mathrm{Re}\{s^2(t)e^{j2\omega_0 t}\} \quad . \tag{3.8}$$ [5)]

The second term at the double frequency is easily filtered out, often already by the detector itself. This means that it is sufficient to study the behaviour of the equivalent low pass signal $s(t)$ to obtain the power.

The propagation of such a pulse $v(t)$ through a linear, time invariant system $h(t)$ is given by the convolution [6)]

$$u(t)e^{j\omega_0 t} = h(t) * \left[s(t)e^{j\omega_0 t}\right] \tag{3.9}$$

which can be rewritten as

$$u(t) = s(t) * \left[h(t)e^{-j\omega_0 t}\right] = s(t) * \hat{h}(t) \tag{3.10}$$

[3)] The physical dimension of field quantities is proportional to $[V_x] \propto \sqrt{\texttt{watts}}$.
[4)] $j = \sqrt{-1}$
[5)] x^* denotes the conjugate complex value of x.
[6)] The convolution is defined by $f(t) * g(t) = \int_{-\infty}^{+\infty} f(\tau)g(t-\tau)\,\mathrm{d}\tau$.

with $\hat{h}(t)$ known as the equivalent low pass system. In the frequency domain (3.10) can be expressed by the multiplication

$$U(\omega) = S(\omega)\hat{H}(\omega) \tag{3.11}$$

with $U(\omega)$ and $S(\omega)$ being the Fourier transforms of the both signals $u(t)$ and $s(t)$.

If $H(\omega)$ is the Fourier transform of $h(t)$

$$H(\omega) = \int_{-\infty}^{+\infty} h(t)e^{-j\omega t}\,\mathrm{d}t \quad , \tag{3.12}$$

the Fourier transform $\hat{H}(\omega)$ of $\hat{h}(t)$ is related to $H(\omega)$ by shifting to ω_0,

$$\hat{H}(\omega) = H(\omega_0 + \omega) \quad . \tag{3.13}$$

Using $H(\omega)$ from (3.5), the equivalent low pass received pulse $u(t)$ can be expressed by the Fourier back-transformation

$$u(t) = \frac{1}{2\pi}\int_{-\infty}^{+\infty} F(\omega_0+\omega)e^{-jk(\omega_0+\omega)2r}S(\omega)e^{j\omega t}\,\mathrm{d}\omega \tag{3.14}$$

To evaluate the integral we make the following observations. Since $S(\omega)$ is narrow band the integral only has substantial contribution for small ω, i.e. $|\omega| \ll \omega_0$. So we invoke the mean value theorem and extract the factor $F(\omega_0 + \omega)$ from the integral. Then we approximate the wave number by the first Taylor term

$$k(\omega_0 + \omega) = k(\omega_0) + k'(\omega_0)\omega \quad . \tag{3.15}$$

We further assume the medium of propagation has negligible loss over the distances of concern meaning $k(\omega_0)$ is almost real valued. Using the approximations, equation (3.14) reads

$$u(t) = F(\omega_0)e^{-j2rk(\omega_0)}\frac{1}{2\pi}\int_{-\infty}^{+\infty} S(\omega)e^{-j\omega 2rk'(\omega_0)}e^{j\omega t}\,\mathrm{d}\omega \tag{3.16}$$

which evaluates to

$$u(t) = F(\omega_0)e^{-j2rk(\omega_0)}s(t - 2rk'(\omega_0)) \tag{3.17}$$

by Fourier back-transformation. The power $p_R(t)$ at the detector output is given by

$$p_R(t) = \frac{1}{2}u(t)u^*(t) = |F(\omega_0)|^2 p_T(t - 2rk'(\omega_0)) \tag{3.18}$$

if we identify the transmit pulse with

$$p_T(t) = \frac{1}{2}s(t)s^*(t) \tag{3.19}$$

re-substitution for $F(\omega_0)$ gives the radar equation for narrow band pulses in a possibly dispersive medium

$$p_R(t) = A_R \frac{G_T(\vec{e_r})}{4\pi r^2}\frac{\sigma_b(\vec{r},\omega_0)}{4\pi r^2} e^{-2\gamma(r,\omega_0)} p_T(t - 2rk'(\omega_0)) \quad . \tag{3.20}$$

From the solution of the MME for harmonic waves it follows, that wave number k is related to frequency ω by means of the dispersion relation

$$k(\omega) = \omega \frac{n(\omega)}{c_0} \tag{3.21}$$

with c_0 the speed of light *in vacuo* and $n(\omega)$ the frequency dependent index of refraction describing the embedding medium. Rearranging Equation (3.21) yields

$$v_{\mathtt{p}}(\omega) = \frac{c_0}{n(\omega)} = \frac{\omega}{k(\omega)} \quad , \tag{3.22}$$

a velocity termed *phase-velocity* determining the speed of a harmonic wave of frequency ω. From the argument of the pulse p_T (a group of harmonic waves) in (3.20) it can be seen, that the velocity of the pulse is given by

$$v_{\mathtt{g}}(\omega) = \left(\frac{\mathrm{d}k}{\mathrm{d}\omega}\right)^{-1} = \frac{c_0}{n(\omega)}\left(1 + \frac{\omega}{n(\omega)}\frac{\mathrm{d}n(\omega)}{\mathrm{d}\omega}\right)^{-1} \quad , \tag{3.23}$$

known as *group-velocity*. It can be seen, that only in a non-dispersive medium, i.e. ,$\frac{\mathrm{d}n}{\mathrm{d}\omega} = 0$, *phase-velocity* and *group-velocity* will be the same.

3.2. Narrow Beam Approximation

In section 3.1 we dealt with backscattering from a single particle. Other scatterers were considered only in terms of their effect on attenuation. For the following we shall assume backscatter from many randomly arranged particles, and we shall further assume that the configuration appears *frozen*, i.e. static, during the doubly round trip time of a single LASER pulse. Under these assumptions where the fields of the scatterers are uncorrelated but fixed[7], we can simply add up their contributions, and equation (3.20) becomes

$$p_R(t) = \int_V A_R \frac{G_T(\vec{e_r})}{4\pi r^2}\frac{\sigma_b(\vec{r},\omega_0)}{4\pi r^2} e^{-2\gamma(r,\omega_0)} p_T(t - 2rk'(\omega_0))\rho(\vec{r})\,\mathrm{d}V \quad . \tag{3.24}$$

The narrow beam approximation means that the pulse energy is concentrated in a narrow cone segment. Then we can assume that the density ρ, the optical distance γ and the backscatter cross section σ_b depend only on the distance r to the sensor and show a negligible lateral variation. If we further assume that the beam interacts in its entirety with the medium, the dependence on the distance is reduced from the fourth to the second power. The volume integration of (3.24), under the narrow beam approximation, can be reduced

[7] In particular this means no Doppler effects from moving particles.

to an integration along only one variable, the range r

$$p_R(t) = \eta \frac{A_R}{4\pi} \int_0^\infty \frac{\sigma_b(r)\rho(r)e^{-2\gamma(r)}}{r^2} p_T(t - \frac{2r}{v_g})\,\mathrm{d}r \tag{3.25}$$

where we have omitted the explicit dependence on ω_0 to make the expressions more readable, have introduced a constant dimensionless scaling factor η to provide for additional unmodeled system losses, and used the group velocity v_g which is the reciprocal of k'. Equation (3.25) is the basis for the remote sensing of properties of the medium. With the definition of system function h

$$h(r) = \eta \frac{A_R}{4\pi} \frac{v_g}{2} \frac{\sigma_b(r)\rho(r)e^{-2\gamma(r)}}{r^2} u(r) \tag{3.26}$$

and variable substitution

$$r = \frac{v_g}{2} t \tag{3.27}$$

equation (3.25) reads

$$p_R(t) = \int_{-\infty}^{+\infty} h(\tau) p_T(t - \tau)\,\mathrm{d}\tau \tag{3.28}$$

as a convolution integral. In (3.26) we have introduced the unit step function $u(r)$, which is one for positive r, and zero else.

The general approach is now to measure $p_R(t)$ and with known $p_T(t)$ to recover $h(t)$, then infer information about the targets from the form of $h(t)$. For the justification of the exponential model used in this thesis the exponential term in (3.26) is of special interest. Assuming that ρ, σ_t, and σ_b are approximately constant, at least in sections, equation (3.26) simplifies to

$$h(t) = u(t) a e^{-gt} \tag{3.29}$$

with

$$g = \rho\sigma_t \frac{v_g}{2}, a = \eta \frac{A_R}{4\pi} \frac{2}{v_g} \frac{\sigma_b \rho}{t_0^2} \tag{3.30}$$

and the approximation of t by constant t_0 which is valid if the distance to the target is much larger than the target spread.

4. Article Summaries

This thesis is a *cummulative work* i.e. it consists of a main body of text and a collection of three *peer reviewed* journal articles and two *conference* contributions which are contained as an appendix at the end. I am the primary author and initiator of all contained articles. N. Pfeifer, head of the research unit of photogrammetry of the TU Wien, co-authored the three peer-reviewed journal articles in his role as the supervisor of this thesis. M. Pfennigbauer my direct superior and colleague at company Riegl, wrote the introduction of a conference paper, helped with proof reading and challenged me with technical discussions. A. Ullrich, chief technical officer at company Riegl helped with proof-reading and discussions for the second article. G. Mandlburger, member of the photogrammetry unit and scientist with very good expertise in ALB, provided reference data for validation, performed an independent second validation, and helped me by asking a number of critical questions. All co-authors helped with proof-reading.

The specific original contributions to ALB within this thesis are

- the introduction of a **waveform model** based on **truncated and shifted exponentials** for use in ALB,
- the use of **truncated exponentials** for the explicit calculation of the convolution between the system waveform (SWFM) and the differential backscatter cross section (dBCS) to obtain the **bathymetric waveform**,
- a method, which I term **exponential decomposition** (XDC) to infer the differential backscatter cross section (dBCS),
- a method to derive the **water surface** from a **single wavelength green** LiDAR system, by identifying it as the leading edge of the decomposed exponential,
- the discovery, that the difference between **group-velocity** and phase-velocity in water is large enough to be an important factor for the **explanation** of **depth bias**.

4.1. System Waveform

The SWFM is the convolution of the outgoing laser pulse with the impulse response of the receiver electronics. The SWFM can be recorded by pointing the range finder of the sensor perpendicularly towards a flat target. In a real system the SWFM can deviate from the "ideal" Gaussian pulse shape, i.e. the shape may be asymmetric and can have a ringing tail induced by the receiver electronics. It is possible to model such a shape as the real part of a sum of complex exponentials, however, standard mathematical procedures fail in determination of the model parameters.

In the first article (Appendix A.1), a conference article, I present a pragmatic engineering solution to the problem and validate the results against measured SWFMs from a range of instruments.

4.2. Exponential Model and Implicit Deconvolution

The received signal from LiDAR can be understood as the convolution of the SWFM and the dBCS. In the bathymetric case a major part of the backscatter is caused by the watercolumn, in particular if the water is turbid. Such backscatter has a pronounced exponential character and suggests a model consisting of a sequence of truncated and shifted exponentials. If also a representation of the SWFM as a sum of exponentials is used, the convolution of such sums of such exponentials with the SWFM can be calculated symbolically. Such a representation of the SWFM has been introduced in article one.

In the second article (Appendix A.2), a peer reviewed journal article, I present the exponential model and give an algorithm to deduce the number and values of parameters from measured data. The effectiveness of the algorithm is demonstrated by application to a real data set.

4.3. Surface and Bottom-Detection

The potential of the model introduced in the second article is not only to find the surface and bottom positions of the water body from the echo waveform of a single wavelength scanner, but also to derive properties of the water column. The algorithm, however, uses a variable number of parameters, increasing the risk of over-fitting. Based on the exponential model of article two I therefore propose a restricted, ten parameters, surface volume bottom (SVB) algorithm.

In the third article (Appendix A.3), a peer reviewed journal article, I investigate the appropriateness and quality of the SVB algorithm, the accuracy of the estimate of the riverbed, and I attempt to find out to which degree it is possible to approach the theoretical limit for target discrimination in very shallow waters. The algorithm is validated against a reference data set that has been acquired by G. Mandlburger, one of the authors, by wading with a pole. The results show good agreement of the bathymetry obtained with the SVB algorithm and the reference. It can be demonstrated that the algorithm is able to resolve depths down to a few cm.

4.4. Depth Measurement Bias

Bias of depth measurement is a still active scientific question. Although, in my third article, I demonstrated that the SVB has virtually no dependence on depth, at least for the very shallow regime, I urged to be careful in generalizing this result, because it is a consequence of choosing a somewhat artificial interpretation of parameters.

In the framework of the MME it is a known fact that the speed of pulses in air is given by the *group velocity*, which is somewhat slower than the speed of continuous harmonic waves which travel with *phase velocity*. This difference in speed, however, is usually negligible in air but amounts to a range error of 1.5% in water, if neglected.

RTT is the standard framework for ALB and since it is based on energetic considerations of harmonic waves it does not consider wave phase explicitly. Consequently the speed of a light pulse must be known a-priori. In all relevant articles I have found, the phase velocity is used for the pulse propagation instead of the group velocity.

In my fourth article (A.4), a peer reviewed journal article, I introduce the consideration of chromatic dispersion as an answer to explain depth error because chromatic dispersion is the reason for the group velocity being different from phase velocity. To the best of my knowledge, the effect of chromatic dispersion in its influence on the propagation velocity has not been considered in the ALB literature so far. In my article I describe and perform an experiment showing that group velocity indeed is different from phase velocity by a relevant amount. I also give a new interpretation of cases of depth bias reported in the literature.

G. Mandlburger's specific contribution was that he tried to cross-validate the laboratory results on field data, and M. Pfennigbauer helped design the experiment.

4.5. Complex Waveforms

One of the obvious consequences of limiting the number of model parameters, as in the SVB algorithm described in my fourth article, is the loss of the ability to account for the complexity of the water column.

In my fifth article (Appendix A.5), a conference article, I demonstrate that LiDAR backscatter from the water column indeed carries information about fine structure. Using a data set obtained in the Hawaiian port of Hilo I am able to show clearly visible patterns of stratification. Since the data set has been obtained with a non-scanning sensor it is possible to visualize it by means of a simple "curtain" representation. In my presentation I also reason about the relationship between the depth of view and the damping coefficient of the exponential segments obtained from the measurement.

5. Discussion

The cumulative character of this thesis means that discussion and conclusion sections are already represented by sections in the accompanying articles A.1, A.2, A.3, A.4, and A.5. In order to avoid being overly repetitive, I will try to pick out those aspects that I think are of interest from a more general perspective. Additionally I will discuss a further refinement of the exponential model.

5.1. Analysis and Processing

The derivation of bathymetry, of course, depends on more than the reconstruction of certain points in time within the received waveform. So must the position and orientation of the sensor at the time the waveform is measured be known. Nevertheless, waveform analysis, as dealt with in this thesis, is only concerned with the determination of these points in time from a single waveform and does not consider information from the spatial neighbourhood of other waveforms. For this reason location and orientation is not needed in the analysis.

There are two instances in time which are of primary importance: The time at which the pulse passes through the water surface and the time at which it hits the bottom. The upper left image of Figure 5.1 shows a textbook like response waveform. The first peak likely is caused by the surface and the second by the bottom. Even in this, at first sight, optimal situation one can raise the question if the small hump after the second peak might be caused by the bottom. In general, there are two ways to find out the truth. The first is to use spatial neighborhood to reason about the true bottom elevation. The methods in this work, however, are restricted to the single shot perspective, needing to resort to the second way. Since the analysis can only use data from a single waveform this method needs to *remove* the effect of the SWFM before estimation to see if the peak is caused by the bottom or not. The top right image in Figure 5.1 shows a model of the waveform that has been fitted almost perfectly to the data. At the bottom left is the XDC of the model, in red color. Since the second hump is caused by the SWFM it does not appear in the decomposed waveform any more. It shall be said that the two peaks are of course not modeled by exponential segments, but as in GDC as Dirac impulses.

Unfortunately the general situation is much more complicated than what Figure 5.1 would suggest.

Figure 5.2 is a small selection of waveforms as they appear in measurements. Aside from the already seen textbook like shape, the case of a strong bottom echo paired with a weaker response from the surface, e.g., as in top right of Figure 5.2, poses the interesting question what causes the increasing part of the waveform between the two peaks.

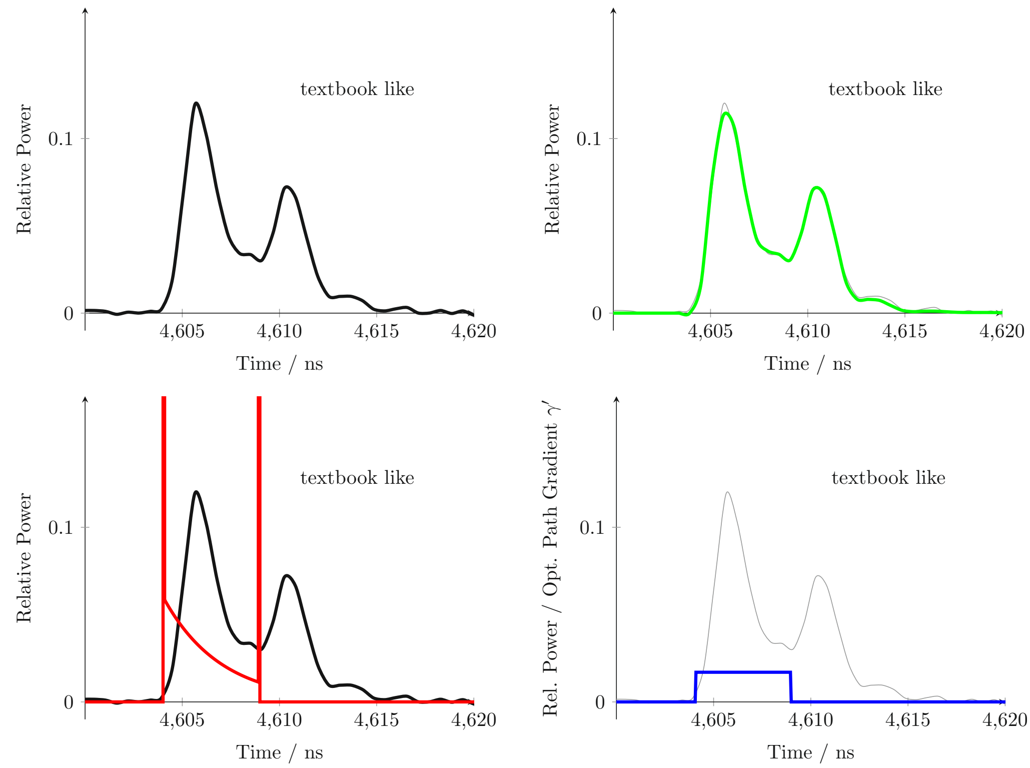

Figure 5.1.: A textbook like waveform, obtained from inland waters. Upper left: raw waveform. Upper right: waveform overlaid by model in green. Lower left: The exponentialy decomposed waveform. Lower right: A possible density distribution which can explain the exponential part.

From a bathymetric perspective this should not really matter, but in reality the presence of this second signal distorts estimation of the ground position. Therefore a model must at least be able to reproduce the disturbing influence so that it can be eliminated. This is the approach I followed in the published articles with success. In an attempt to show future directions, however, I will try to sketch a model that goes beyond and that could provide an explanation, for such effects as the slowly raising segment.

If it is assumed that σ_t and σ_b can be treated as constant, meaning that the change in attenuation is caused by density variations alone, we can see from (3.2) that the density can be expressed as

$$\rho(r) = \frac{1}{\sigma_t}\gamma'(r) \tag{5.1}$$

and (3.26) becomes

$$h(r) = \eta \frac{A_R}{4\pi}\frac{v_g}{2}\frac{\sigma_b}{\sigma_t}\frac{1}{r^2}\gamma'(r)e^{-2\gamma(r)}u(r) \quad . \tag{5.2}$$

If it is further assumed that the density ρ also is constant within layers of different depth,

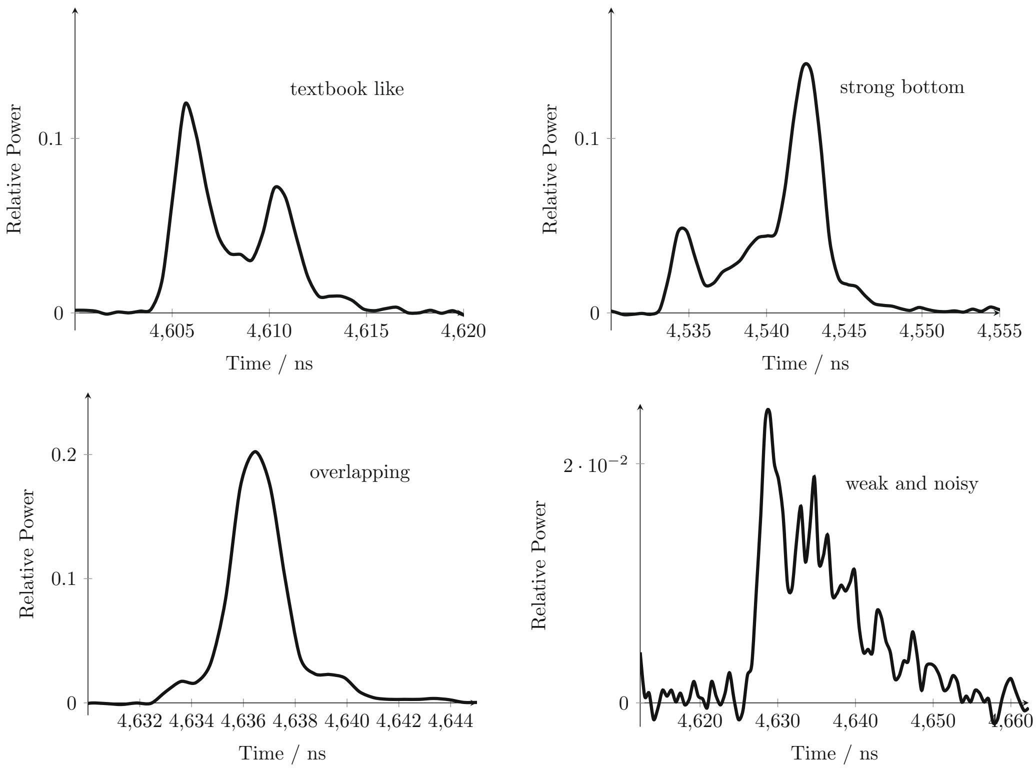

Figure 5.2.: A small selection of waveforms, demonstrating the variety of shapes.

then we can use the following exponential model

$$h(r) = A \sum_{I} u(r - r_i) \gamma'_i e^{-\gamma'_i 2(r-r_i)} \tag{5.3}$$

where $\gamma'_i = \sigma_t \rho_i$ and A is a single scaling parameter that combines the other constants

$$A = \eta \frac{A_R}{4\pi} \frac{v_g}{2} \frac{\sigma_b}{\sigma_t} \frac{1}{r_0^2} \quad .$$

The lower right image of Figure 5.3 shows an optical path density gradient γ' that can explain the raising behaviour. Figure 5.4 shows similar results for the other cases. The determination of a suitable algorithm to find the parameters automatically, however, has to be postponed into the future.

The processing of the signals, the XDC proceeds in two phases. First a good enough set of initial values for the parameters has to be found, and then a constrained non-linear fit must be performed. Finding the initial parameters is all the more difficult as the variety of signal shapes increases. The problem is even more severe if the algorithm is supposed to work blind, i.e. no a priori knowledge about land or water is available. As a preparatory step, an approximate land-water delimitation was therefore used, since the processing times of the algorithm otherwise would have been extremely long due to the superfluous analysis

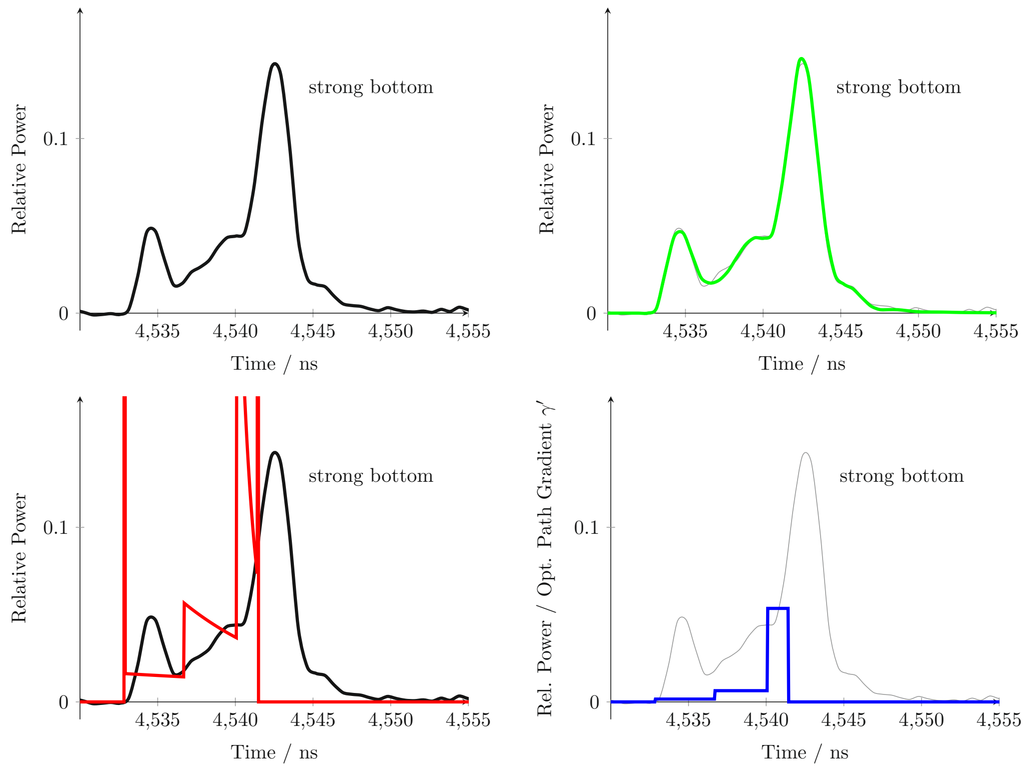

Figure 5.3.: Can a increasing density, as seen on the lower right, explain the raising segment between the peaks?

attempts of the land mass.

The chosen description of the signals by truncated exponentials has shown speed advantages compared to discrete signal processing, especially because the convolution operation can be performed more efficiently. Nevertheless, if the method shall be used for processing mass data, it must be made even more efficient.

5.2. Single Wavelength ALB

IR LiDAR does not penetrate into the water. This is why it can be used to detect the water surface reliably. A scanner for ALB, however, is not only more complex because of the need for a second LASER with a wavelength in the visible region, e.g. a green LASER, but also potentially will suffer from the following problem: Ideally, the two beams, green and infrared, would be collinear. For small off-nadir angles the IR signal delivers good response from the surface, but at the same time will the green signal. Unfortunately a strong green return means severely reducing receiver sensitivity for the signal from just behind for an certain amount of time. Consequently, it is tried to eliminate surface echoes when wanting to capture echos from below the water surface to increase sensitivity. This is one of the reasons why the green LASER is typically operated at a constant ≈ 20° off-nadir angle.

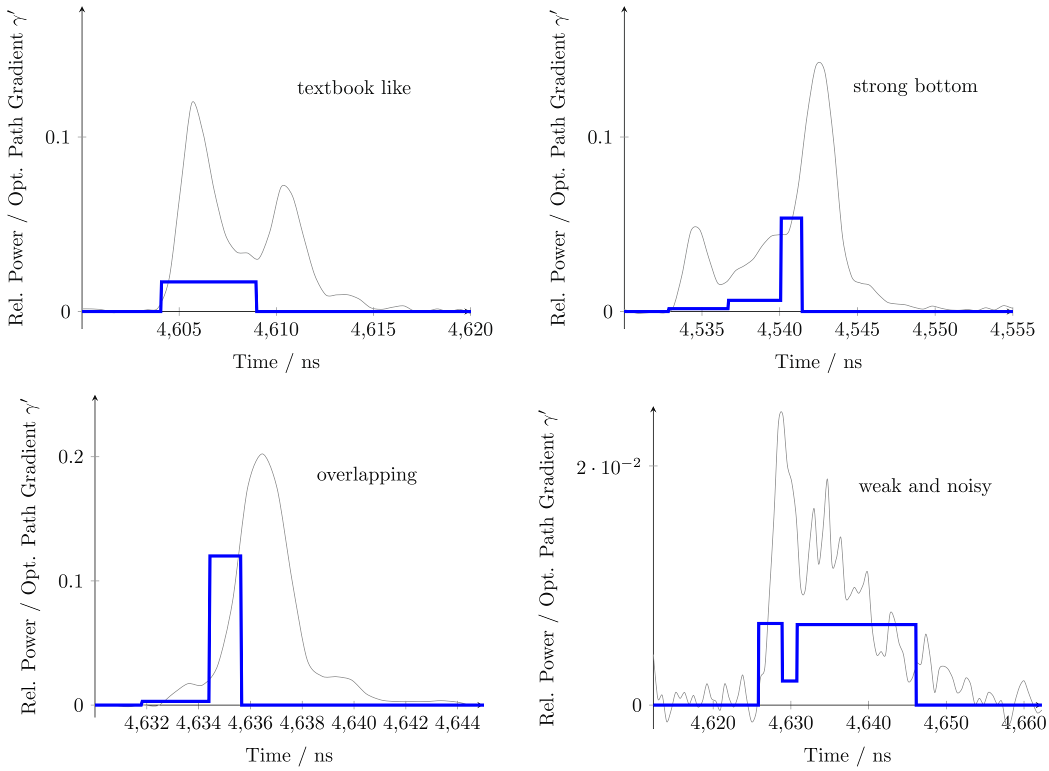

Figure 5.4.: Piecewice constant optical path gradients possibly can *explain* the behavior of the shown waveforms.

Operating the IR LASER at the same angle obviously is not without problems because at this angle specular reflections tend to reduce the receivable echo amplitude. For this reason it seems advantageous if the water surface can be directly derived from the green response alone, eliminating the need for the IR LASER.

Wang et al. [32] have evaluated six algorithms on single-wavelength bathymetric signals which were designed for the topographic case. While all the methods are reported to be usable to a certain degree, the results are mainly based on a simulated dataset and for the measured dataset no reference data is reported. Since all methods for topographic use basically are detection methods for discrete positions, often visible in the waveform as peaks there is a fundamental problem for bathymetric use. The peak from the green response, will occur from *below* the surface, because it is the result of the convolution of the SWFM and the particles in the water column and will cause a systematic depth error.

If the exponential model is valid, and our findings indicate that it is, the leading edge of the (truncated) exponential coincides with the water surface thereby avoiding the depth error. The direct validation against IR LASER data could not be performed without gaps in this work, but shows good results in the zones of overlap.

An indirect validation if the surface has been found correctly is by checking that the ground points have been determined correctly by comparing them to a reference set.

Although this test was positive in this work, the result is related to the open question of the depth-dependent error which will be discussed later.

5.3. Minimum Depth

The question about the minimum detectable depth can be viewed from different perspectives. From the application perspective the question seems to be clear at first sight, although the question may either be about the dividing line between land and water or whether there is a water-covered surface at all, such as in swampy areas.

Approaching the question from the sensor perspective one may find definitions, like the one given by Legleiter et al. [14]

$$\Delta h = \frac{1}{2} c_w \Delta t cos(\theta_w) \tag{5.4}$$

relating the minimum depth Δh to the speed of light in water c_w, the sampling time intervall Δt, and the angle of incidence θ_w. Such definitions typically need to make additional assumptions about the detection scheme. In the cited case it is assumed that at least two peaks must be detectable in the waveform. If the detection scheme is different, as in GDC or XDC, two separable peaks are not a requirement. In the case of GDC it is required that two closely spaced Gaussians be distinguishable from a single Gaussian. The ability to do so will depend on the amount of noise present since in the noise-free case two Gaussians may be located arbitrarily close and still remain distinguishable. In the case of the SVB algorithm of paper A.3, there will always be a surface and a bottom, because the behaviour is built into the model.

Finally, one can discuss the question about the minimum detectable depth from the point cloud perspective. In the latter case, the question is one of the ability to distinguish between two layers of point clouds and determine their mutual distance.

For this work the signed distance between two point clouds has been used. The two clouds were previously classified according to surface and ground points in a semi-automatic process. It could be demonstrated, that for the SVB algorithm the distances continuously approach zero.

Two remarks remain to be made, however. Firstly this result must not be misinterpreted as an ability of the SVB algorithm to detect the presence of water surfaces. Secondly, the result is somewhat relativized by the fact that the need for refraction correction decreases near the banks, because the errors are no longer significant if refraction correction is omitted completely in these areas. Consequently, as far as the question of the terrain model is concerned, it is not important at which depth the water surface can no longer be detected.

5.4. Depth Bias

The measurement of the water depth by means of light propagation depends first of all on the ability to determine from the backscattered waveform two distinguished points which can be attributed to the surface and the bottom. Then, of course, the accuracy of the clock with which the time instants of the two designated points are determined will also play a major role. Thirdly, the speed of light as it propagates in water will affect the result of the measurement because it directly determines the conversion factor between time and range.

It is the first of these three factors that has been most discussed so far, and which also has the greatest influence on measurement error. The second factor, the accuracy of the time measurement, can be regarded as secondary in the current state of the art. But what has not been questioned so far is the third factor, the speed itself.

It is a well known fact that light undergoes a change of direction when it enters into the water. This change of direction is determined by the relative speeds in air and water and is given by the ratio of the refractive indices of the two media.

It is also a known fact that pulsed light propagation in air occurs with group velocity, which is slightly smaller than the phase velocity. The difference in velocity is by a factor of $1 + 3 \times 10^{-4}$, so it is usually neglected for distance measurement.

It is just as true that light pulses in water propagate slightly slower than with phase velocity, the speed which is given as the ratio of the speed of ligth in vacuo and the refractive index. Within the ALB community, however, the magnitude of this slow down, amounting to 1.5%, has been underestimated. Especially in clear water, where the effect of pulse broadening is smaller, the effect of group delay explains very well the observed depth measurement errors. Although it is not expected that accounting for group velocity will completely avoid the systematic depth error, the considerations given in my fourth article (A.4) show that a significant part is due to its neglect. I must not miss mentioning that a first look at recent measurements, indicate that especially in turbid water, the proportional depth error cannot be explained by considering group velocity alone.

6. Conclusions

Analysis: In this thesis I have introduced a novel, to the best of my knowledge, *exponential* model for the waveforms of backscatter from bathymetric LiDAR. The first part of the model is a description of the dBCS as a chain of truncated exponential segments and idealized pointlike Dirac pulses, which can be expressed as a sum. The second part of the model is a representation of the measured SWFM as the real part of a sum of complex truncated exponentials. The model differs from other existing exponential models in that *time-shifted* exponential segments are used to describe the non-pointlike parts of the dBCS. Since the convolution of the both sums, dBCS and SWFM, can be carried out analytically, various continuous model variants with physically meaningful parameters can be crafted. In paper A.2 I have used the method to define a model of a variable number of exponentials to describe generic response waves, in paper A.3 I have used the method to define the more restricted SVB model. In both cases, the resulting models allow a faithful representation of the data.

Processing: The model of bathymetric backscatter LiDAR waveforms, introduced in this thesis is a parametric one. The parameters of the SWFM are determined during system calibration and remain fixed afterwards. The parameters of the dBCS are evaluated during data processing and result in an XDC of the dBCS.

The parameters can be found by solving a non-linear lest squares problem. Unfortunately there is no robust method for finding good start parameters that works for the general case, since the shapes of the waveforms can be very diverse. Nevertheless, in paper A.3 I described a procedure that worked sufficiently for the data which has been measured at a tributary of the Danube River. The results compared to a set of reference points obtained by a global navigation satellite system (GNSS) with a standard deviation of the error of 3 cm.

Although the use of truncated exponentials allows an efficient implementation of the convolution operation, the method does not yet seem to be fast enough for real-time processing.

Questions covered: The answer to the question whether a *single wavelength* system is feasible has an impact on the complexity of the LiDAR. The use of the leading edge of the XDC is a more robust and unbiased estimate of the water surface, see papers A.2, A.3, than the use of the position of the peak from the water column. So, while the answer *yes* to the question is not new, using the leading edge of the XDC will make such a system more reliable.

It turns out that the question of resolvable *minimum depth* is not as clear as it may appear at first glance. For this thesis I took a pragmatic point of view using the signed difference of two pointclouds that have been classified as surface and bottom. As discussed in paper A.3 it turns out that the SVB algorithm seamlessly approaches zero depth, although this mustn't be misinterpreted as the ability of the method to detect puddle-like water.

The question about the *speed of light in water* is also a question about the depth measurement error caused by neglecting the effect of chromatic dispersion that occurs with pulsed light. The effect is present in air as well, but can usually be neglected in air because of its small magnitude. Neglecting the effect in water will cause a depth proportional error of about 1.5 %. Because the effect of group velocity has not been discussed in the ALB literature, despite its magnitude, and already occurs in clear water, in paper A.4 I describe an experiment that I have performed. I further show that the effect can describe depth errors for which no explanation could be given in the literature. While I could show, that the group velocity, especially in clear water, can adequately describe the depth dependent error, there seems to be little doubt, that in turbid water further effects have to be considered to eliminate the error completely.

A. Published Articles

A.1. Finding model parameters for the system waveform of a full-wave lidar: a pragmatic solution [26]

Type: Conference contribution.

Status: Published October 10, 2018.

Embedded version: Manuscript accepted for publication.

Bibliography: Roland Schwarz and Martin Pfennigbauer. "Finding model parameters for the system waveform of a full-wave lidar: a pragmatic solution." In: *Remote Sensing of the Ocean, Sea Ice, Coastal Waters, and Large Water Regions 2018.* Ed. by Charles R. Bostater, Stelios P. Mertikas, and Xavier Neyt. SPIE, Oct. 2018. DOI: 10.1117/12.2323965

Author contributions: R. Schwarz had the idea, implemented the method, wrote the article, and presented the topic at conference: SPIE Remote Sensing, 2018, Berlin, Germany. M. Pfennigbauer was project manager, had the supervision and performed the proof reading.

Support of the study: RIEGL Research Forschungsgesellschaft mbH, 3580 Horn, Austria

Pages from 30 to 37 have been omitted from the online version to comply with copyright requirements.

A.2. Exponential Decomposition with Implicit Deconvolution of Lidar Backscatter from the Water Column [29]

Type: Peer reviewed journal article.

Status: Accepted April 26, 2017, published July 6, 2017.

Embedded version: Manuscript accepted for publication.

Bibliography: Roland Schwarz et al. "Exponential Decomposition with Implicit Deconvolution of Lidar Backscatter from the Water Column." In: *PFG – Journal of Photogrammetry, Remote Sensing and Geoinformation Science* 85.3 (July 6, 2017), pp. 159–167. ISSN: 2512-2789, 2512-2819. DOI: 10.1007/s41064-017-0018-z

Author contributions: R. Schwarz had the idea, implemented the method, wrote the article, and handled the peer review. N. Pfeifer was the supervisor and did the proof reading. M. Pfennigbauer obtained the scanner data sets, was the contact person for the contextual project *Alpine Airborne Hydro Mapping*, and did the proof reading. A. Ullrich was the technical head and did the proof reading.

Support of the study: RIEGL Research Forschungsgesellschaft mbH, 3580 Horn, Austria

A.3. Design and Evaluation of a Full-Wave Surface and Bottom-Detection Algorithm for LiDAR Bathymetry of Very Shallow Waters [28]

Type: Peer reviewed journal article.

Status: Accepted February 8, 2019, published April 1, 2019, received the 2019 U.V. Helava Best Paper Award 10.1016/j.isprsjprs.2020.03.015

Embedded version: Manuscript accepted for publication.

Bibliography: Roland Schwarz et al. "Design and evaluation of a full-wave surface and bottom-detection algorithm for LiDAR bathymetry of very shallow waters." In: *ISPRS Journal of Photogrammetry and Remote Sensing* 150 (Apr. 2019), pp. 1–10. DOI: 10.1016/j.isprsjprs.2019.02.002

Author contributions: R. Schwarz had the idea, implemented the method, performed the data processing, wrote the article, and handled the peer review. G. Mandlburger provided the reference data set, performed a second independent performance assessment for cross-validation, and did the proof reading. M. Pfennigbauer was the project leader and did the proof reading. N. Pfeifer was the supervisor and did the proof reading.

Support of the study: RIEGL Research Forschungsgesellschaft mbH, 3580 Horn, Austria and German Research Foundation (DFG) project 'Bathymetry by fusion of airborne laser scanning and multispectral imagery'.

Pages from 51 to 62 have been omitted from the online version to comply with copyright requirements.

ISPRS Journal of Photogrammetry and Remote Sensing 164 (2020) 171–172

Contents lists available at ScienceDirect

ISPRS Journal of Photogrammetry and Remote Sensing

journal homepage: www.elsevier.com/locate/isprsjprs

Announcement

The U. V. Helava Award – Best Paper Volumes 147-158 (2019)

Derek Lichti (Editor-in-Chief)

ISPRS Journal of Photogrammetry and Remote Sensing, The University of Calgary

The U.V. Helava Award, sponsored by Elsevier B.V. and Leica Geosystems AG, is a prestigious ISPRS Award that was established in 1998 to encourage and stimulate submission of high quality scientific papers by individual authors or groups to the ISPRS Journal of Photogrammetry and Remote Sensing, to promote and advertise the Journal, and to honour the outstanding contributions of Dr. Uuno V. Helava to research and development in photogrammetry and remote sensing.

The Award is presented to authors of the best paper, written in English and published exclusively in the ISPRS Journal of Photogrammetry and Remote Sensing during the four-year period from January of a Congress year, to December of the year prior to the next Congress. The Award consists of a monetary grant of SFr. 10,000 and a plaque. A five-member Jury, comprising experts of high scientific standing, whose expertise covers the main topics included in the scope of the Journal, evaluates the papers. For each year of the four-year evaluation period, the best paper is selected, and among these four papers, the one to receive the U.V. Helava Award will be selected.

The U.V. Helava Award will be presented at the 24th ISPRS Congress in Nice, France, 14-20 June 2020. The Jury appointed by the ISPRS Council, evaluated papers from volumes 147-158 (2019) and announces its decision for the Best Paper. The winner of the 2019 Best Paper Award is:

"Design and evaluation of a full-wave surface and bottom-detection algorithm for LiDAR bathymetry of very shallow waters" by Roland Schwarz [a,b], Gottfried Mandlburger [b,c], Martin Pfennigbauer [a] and Norbert Pfeifer [b].

[a] Riegl Research, Austria
[b] Technische Universität Wien, Austria
[c] University of Stuttgart, Germany

published in volume 150, April 2019, pp. 1-110 https://www.sciencedirect.com/science/article/pii/S0924271619300358

Roland Schwarz

Gottfried Mandlburger

Martin Pfennigbauer

Norbert Pfeifer

E-mail address: ddlichti@ucalgary.ca.

https://doi.org/10.1016/j.isprsjprs.2020.03.015

Available online 11 May 2020
0924-2716

Jury's rationale for the paper selection

This paper presents a new contribution to multimedia lidar methodology for shallow water bathymetric mapping. The authors' SVB (surface, volume and bottom) algorithm represents a new, innovative contribution to underwater topographic mapping. A considerable advantage of their method is that it relies only on a single laser wavelength. The Jurors were impressed with the detailed modelling of the return waveform, the clarity of the explanation, the convincing experimental results and potential for broader applicability of the method.

On behalf of the ISPRS and the U.V. Helava Award Jury, I would like to congratulate the authors for this distinction and thank them for their contribution. I also hank the sponsors of the Award and the Jury members for their thorough evaluations.

A.4. Depth Measurement Bias in Pulsed Airborne Laser Hydrography Induced by Chromatic Dispersion [27]

Type: Peer reviewed journal article.

Status: accepted June 12, 2020, published June 30, 2020

Embedded version: Manuscript accepted for publication.

Bibliography: Roland Schwarz et al. "Depth Measurement Bias in Pulsed Airborne Laser Hydrography Induced by Chromatic Dispersion." In: *IEEE Geoscience and Remote Sensing Letters* (2020), pp. 1–5. DOI: 10.1109/lgrs.2020.3003088

Author contributions: R. Schwarz had the idea, designed and performed the experiment, evaluated the experimental data, wrote the article, and handled the peer review. M. Pfennigbauer was the project leader, helped design the experiment, and did the proof reading. N. Pfeifer was the supervisor and did the proof reading. G. Mandlburger tried to validate the findings on field data and did the proof reading.

Support of the study: RIEGL Research Forschungsgesellschaft mbH, 3580 Horn, Austria; Austrian Research Funding Agency (FFG) within project "Aerial search & Rescue support and supErvision of inAccessible terrainS" (AREAS) 86702; German Research Foundation (DFG) for project SO 9356/6-1.

Pages from 66 to 70 have been omitted from the online version to comply with copyright requirements.

A.5. Detailed Analysis of Complex Waveforms of a UAV Laser Bathymeric Profiler [25]

Type: Conference contribution.

Status: Accepted February 18, 2019.

Embedded version: German: Manuscript accepted for publication. English: Translated by Roland Schwarz after publication.

Bibliography: Roland Schwarz and Martin Pfennigbauer. "Detaillierte Analyse komplexer Wellenformen eines UAV Laser Bathymetrie Profilmessgerätes." In: *Publikationen der deutschen Gesellschaft für Photogrammetrie, Fernerkundung und Geoinformation e.V. Band 28*. 2019. URL: https://www.dgpf.de/src/tagung/jt2019/proceedings/proceedings/papers/77_3LT2019_Schwarz_Pfennigbauer.pdf

Author contributions: R. Schwarz formulated the model, did the analysis and data processing, wrote the main body of the article, presented the topic at conference: "Dreiländertagung der DGPF, der OVG und der SGPF in Wien", 2019. M. Pfennigbauer was the project leader, wrote the introduction, and did the proof reading.

Support of the study: RIEGL Research Forschungsgesellschaft mbH, 3580 Horn, Austria.

Pages from 72 to 100 have been omitted from the online version to comply with copyright requirements.

Bibliography

[1] Lydia Abady et al. "Assessment of Quadrilateral Fitting of the Water Column Contribution in Lidar Waveforms on Bathymetry Estimates." In: *IEEE Geoscience and Remote Sensing Letters* 11.4 (Apr. 2014), pp. 813–817. ISSN: 1545-598X. DOI: 10.1109/lgrs.2013.2279271.

[2] H. Abdallah et al. "Potential of Space-Borne LiDAR Sensors for Global Bathymetry in Coastal and Inland Waters." In: *IEEE Journal of Selected Topics in Applied Earth Observations and Remote Sensing* 6.1 (Feb. 2013), pp. 202–216. DOI: 10.1109/jstars.2012.2209864.

[3] Seibert Q. Duntley. "Light in the Sea*." In: *Journal of the Optical Society of America* 53.2 (Feb. 1, 1963), p. 214. DOI: 10.1364/josa.53.000214. URL: https://www.osapublishing.org/abstract.cfm?URI=josa-53-2-214.

[4] Gary C. Guenther. *Airborne laser hydrography system design and performance factors*. Technical Guide. National Ocean Service,Charting and Geodetic Services, Rockville, MD,20852, 1985. URL: http://www.dtic.mil/cgi-bin/GetTRDoc?Location=U2%5C&doc=GetTRDoc.pdf%5C&AD=ADA488936.

[5] Kai Guo et al. "Gaussian Half-Wavelength Progressive Decomposition Method for Waveform Processing of Airborne Laser Bathymetry." In: *Remote Sensing* 10.1 (Dec. 2017), p. 35. DOI: 10.3390/rs10010035.

[6] G. Daniel Hickman and John E. Hogg. "Application of an airborne pulsed laser for near shore bathymetric measurements." In: *Remote Sensing of Environment* 1.1 (Mar. 1969), pp. 47–58. DOI: 10.1016/s0034-4257(69)90088-1.

[7] Matúš Hodúl et al. "Satellite derived photogrammetric bathymetry." In: *ISPRS Journal of Photogrammetry and Remote Sensing* 142 (Aug. 2018), pp. 268–277. DOI: 10.1016/j.isprsjprs.2018.06.015.

[8] Hydrographic Dictionary Working Group. *Hydrographic Dictionary*. International Hydrographic Organization. URL: http://iho-ohi.net/S32/ (visited on 09/03/2020).

[9] Hydrographic Office. *The United Kingdom Hydrograhic Office - History*. 2013. URL: https://web.archive.org/web/20131114015451/http://www.ukho.gov.uk/AboutUs/Documents/timeline.pdf (visited on 09/05/2020).

[10] Akira Ishimaru. *Wave Propagation and Scattering in Random Media*. Wiley-IEEE Press, 1978. ISBN: 0-7803-4717-X.

[11] Iosif L. Katsev et al. “Efficient technique to determine backscattered light power for various atmospheric and oceanic sounding and imaging systems.” In: *Journal of the Optical Society of America A* 14.6 (June 1997), p. 1338. DOI: 10.1364/josaa.14.001338.

[12] Minsu Kim et al. “Modeling of Airborne Bathymetric Lidar Waveforms.” In: *Journal of Coastal Research* 76 (Dec. 2016), pp. 18–30. DOI: 10.2112/si76-003.

[13] Yuri I. Kopilevich, Viktor I. Feygels, and Alexey I. Surkov. “Mathematical modeling of input signals for oceanographic lidar systems.” In: *Ocean Remote Sensing and Imaging II*. Ed. by Robert J. Frouin, Gary D. Gilbert, and Delu Pan. SPIE, Nov. 2003, p. 30. DOI: 10.1117/12.506980. URL: http://proceedings.spiedigitallibrary.org/proceeding.aspx?doi=10.1117/12.506980 (visited on 06/08/2017).

[14] Carl J. Legleiter et al. “Evaluating the capabilities of the CASI hyperspectral imaging system and Aquarius bathymetric LiDAR for measuring channel morphology in two distinct river environments.” In: *Earth Surface Processes and Landforms* 41.3 (Oct. 2015), pp. 344–363. DOI: 10.1002/esp.3794.

[15] Hans-Gerd Maas. “On the Accuracy Potential in Underwater/Multimedia Photogrammetry.” In: *Sensors* 15.8 (July 2015), pp. 18140–18152. DOI: 10.3390/s150818140.

[16] Aleksey V. Malinka and Eleonora P. Zege. “Analytical modeling of Raman lidar return, including multiple scattering.” In: *Applied Optics* 42.6 (Feb. 2003), p. 1075. DOI: 10.1364/ao.42.001075.

[17] Clément Mallet and Frédéric Bretar. “Full-waveform topographic lidar: State-of-the-art.” In: *ISPRS Journal of Photogrammetry and Remote Sensing* 64.1 (Sept. 2008). bibtex: mallet_full-waveform_2008, pp. 1–16. ISSN: 09242716. DOI: 10.1016/j.isprsjprs.2008.09.007. URL: http://linkinghub.elsevier.com/retrieve/pii/S0924271608000993 (visited on 03/28/2016).

[18] G. Mandlburger, M. Pfennigbauer, and N. Pfeifer. “Analyzing near water surface penetration in laser bathymetry - A case study at the River Pielach.” In: *ISPRS Annals of Photogrammetry, Remote Sensing and Spatial Information Sciences* II-5/W2 (Oct. 2013), pp. 175–180. DOI: 10.5194/isprsannals-ii-5-w2-175-2013.

[19] Michael I. Mishchenko. “Directional radiometry and radiative transfer: The convoluted path from centuries-old phenomenology to physical optics.” In: *Journal of Quantitative Spectroscopy and Radiative Transfer* 146 (Oct. 2014), pp. 4–33. DOI: 10.1016/j.jqsrt.2014.02.033.

[20] Ocean Exploation and Research. *Historical Timeline*. 2020. URL: https://oceanexplorer.noaa.gov/history/timeline (visited on 09/05/2020).

[21] Athanasios Papoulis. *Signal analysis*. New York: McGraw-Hill, 1977. ISBN: 0070484600.

[22] William Philpot. *Airborne Laser Hydrography II*. 2019. DOI: 10.7298/jxm9-g971. URL: https://hdl.handle.net/1813/66666 (visited on 09/11/2020).

[23] F.C. Polcyn, W.L. Brown, and I.J. Sattinger. *The Measurement of Water Depth by Remote Sensing Techniques*. 8973-26-F. Willow Run Laboratories, The University of Michigan, Ann Arbor, 1970. URL: https://apps.dtic.mil/sti/pdfs/AD0714001.pdf (visited on 09/08/2020).

[24] Mikhail N. Polyanskiy. *Refractive index database*. 2020. URL: https://refractiveindex.info (visited on 09/06/2020).

[25] Roland Schwarz and Martin Pfennigbauer. "Detaillierte Analyse komplexer Wellenformen eines UAV Laser Bathymetrie Profilmessgerätes." In: *Publikationen der deutschen Gesellschaft für Photogrammetrie, Fernerkundung und Geoinformation e.V. Band 28*. 2019. URL: https://www.dgpf.de/src/tagung/jt2019/proceedings/proceedings/papers/77_3LT2019_Schwarz_Pfennigbauer.pdf.

[26] Roland Schwarz and Martin Pfennigbauer. "Finding model parameters for the system waveform of a full-wave lidar: a pragmatic solution." In: *Remote Sensing of the Ocean, Sea Ice, Coastal Waters, and Large Water Regions 2018*. Ed. by Charles R. Bostater, Stelios P. Mertikas, and Xavier Neyt. SPIE, Oct. 2018. DOI: 10.1117/12.2323965.

[27] Roland Schwarz et al. "Depth Measurement Bias in Pulsed Airborne Laser Hydrography Induced by Chromatic Dispersion." In: *IEEE Geoscience and Remote Sensing Letters* (2020), pp. 1–5. DOI: 10.1109/lgrs.2020.3003088.

[28] Roland Schwarz et al. "Design and evaluation of a full-wave surface and bottom-detection algorithm for LiDAR bathymetry of very shallow waters." In: *ISPRS Journal of Photogrammetry and Remote Sensing* 150 (Apr. 2019), pp. 1–10. DOI: 10.1016/j.isprsjprs.2019.02.002.

[29] Roland Schwarz et al. "Exponential Decomposition with Implicit Deconvolution of Lidar Backscatter from the Water Column." In: *PFG – Journal of Photogrammetry, Remote Sensing and Geoinformation Science* 85.3 (July 6, 2017), pp. 159–167. ISSN: 2512-2789, 2512-2819. DOI: 10.1007/s41064-017-0018-z.

[30] David J. Segelstein. "The Complex Refractive Index of Water." MA thesis. University of Missouri-Kansas City, 1981. 174 pp.

[31] Merrill Ivan Skolnik. *Introduction to radar systems*. 2nd ed. Singapore: McGraw-Hill Book Co, 1981. 581 pp. ISBN: 0-07-Y66572-9.

[32] Chisheng Wang et al. "A comparison of waveform processing algorithms for single-wavelength LiDAR bathymetry." In: *ISPRS Journal of Photogrammetry and Remote Sensing* 101 (Mar. 2015), pp. 22–35. ISSN: 0924-2716. DOI: 10.1016/j.isprsjprs.2014.11.005. URL: https://www.sciencedirect.com/science/article/pii/S0924271614002718 (visited on 01/29/2017).

[33] Shuai Xing et al. "A Depth-Adaptive Waveform Decomposition Method for Airborne Lidar Bathymetry." In: *Sensors* (2019). DOI: 10.3390/s19235065.

Roland Schwarz

Curriculum Vitae

Zur Person

Name:	Dipl. Ing. Roland Schwarz
Geburtsdatum:	1961-03-23
Familienstand:	verheiratet
Ehefrau:	Karin Straub
Staatsangeh.:	Österreich

Ausbildung

2014–heute **Studium**, *Technische Universität*, Wien.
Dr.-Studium der techn. Wissenschaften Vermessung und Geoinformation

1979–1997 **Diplom Ingenieur**, *Technische Universität*, Wien.
Elektrotechnik - Nachrichtentechnik

1971–1979 **Matura**, *AHS Kundmanngasse*, Wien.

Beruflicher Werdegang

1992–heute **Sen. Research Assistent**, RIEGL LMS GesmbH, Horn.
- Forschung und Entwicklung
- Software und Firmware Produktion
- Technische Kundenbetreuung

1988–1992 **Angestellter im EDV Bereich**, *Div. Arbeitgeber*, Wien.
- Fa. Mesonic - Buchhaltungssoftware
- Fa. Moor - Lackner - Telekom Produkte
- Fa. ISYS - Selbstbau und Microcomputersysteme

vor 1988 Verschiedene Studentenjobs zur Unterstützung der Finanzierung des Studiums